

# Linear Photometric Stereo using Close Lighting Images based on Intensity Differential

Zennichiro Sasaki, Fumihiko Sakaue and Jun Sato

*Nagoya Institute of Technology, Nagoya, Japan*  
{sasaki@cv., sakaue@, junsato@}nitech.ac.jp

**Keywords:** Photometric Stereo, Surface Normal Reconstruction, Close Light Source.

**Abstract:** In this paper, we propose a new linear photometric stereo method from images taken under close light sources. When an images are taken under close light source, we can obtain not only surface normal but also shape from the images. However, relationship between observed intensity and object shape is not linear, and then, we have to use non-linear optimization to estimate object shape. In order to estimate object shape by just linear estimation, we focus not only direct observed intensities, but also differentials of the intensities in this paper. By using the set of observed intensity and its differentials, we can represent relationship between object shape and intensities linearly. By this linear representation, linear estimation of object shape achieved even if obtained images are taken under close light sources. Experimental results show our proposed method can reconstruct object shape by only linear estimation efficiently and accurately.

## 1 INTRODUCTION

Object shape reconstruction from camera images is one of the most important problem in field of computer vision. Especially, shape reconstruction taken under different lighting environment, so called photometric stereo(Woodham, 1980), is useful for applying to research on Computer Graphics (CG) and Virtual Reality (VR) since the method can directly reconstruct surface normal which is important for rendering image. Therefore, this kind of methods are widely studied and practically used(Chen et al., 2011; Brostow et al., 2011) recently.

In the traditional photometric stereo method, there are two strong assumptions. The first assumption is related to reflection and it assumed that reflection on the object surface can be described by Lambert (diffuse) reflection model. The second assumption is for light sources and it assumed that a light source is placed on infinite point in the scene. In order to relax these assumptions, many kinds of methods are proposed. However, effect of first assumption relaxation is limited since most of the object surface can be approximately represented by Lambert model. Of course although specular reflection such as hi-light cannot be represented by this model, effect of them is in limited case. For example, specular reflection by Phong model can be observed only when a viewpoint is on specular direction of a light source. That is, this

kind of reflection cannot be observed from most of the viewpoints.

On the other hand, set up of light source by second assumption includes serious problem. If light source is placed at not infinite point but close to the object, light source direction of each point on the surface changes drastically. In this case, surface normal cannot be estimated correctly. Therefore, we have to maintain large space to utilize photometric stereo. In order to avoid this problem, several methods which use a close point light source are proposed(Iwahori, 1990; Kim and Burger, 1991; Okabe and Sato, 2006; Hayakawa, 1994). In these methods, distance between the point light source and the target object is near, and then, it is not necessary to prepare a large space. Furthermore, these methods can obtain additional information which is lost in images taken under an infinite point light source. That is, these images include not only surface normal information, but also object shape information. Therefore, object shape can be reconstructed directly by the methods. However, since relationship between observed intensities and object shape is non-linear, these methods require non-linear optimization which requires large computational cost.

In order to avoid this problem, linear shape estimation methods are proposed(Fujita et al., 2009; Kato et al., 2010). Although these methods can reconstruct object shape and surface normal by only linear esti-

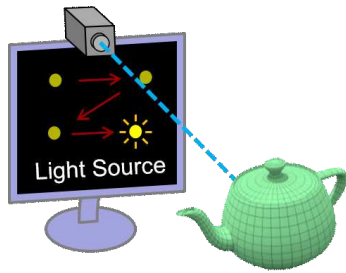


Figure 1: Video display device as a set of light sources. By using the display, position of light source can be controlled easily and quickly.

mation, they used approximated intensity model, and then, accuracy of these methods are not better. Therefore, more accurate linear representation is required for effective object shape estimation. In this paper, we propose a new linear shape reconstruction method using images taken under close light source without any approximation. For this objective, we focus not only observed images, but also differentials of the observed images. In addition, we propose a compact shape estimation system based on the proposed shape reconstruction method. In this system, we use a video display as a set of light sources as shown in Fig.1. By using the display, position of light source can be controlled easily and quickly. In order to use the system we need to describe intensity model including lighting characteristic of the display since this characteristics depends on products. By using our proposed method and this system, we measure the object shape efficiently and accurately.

## 2 INTENSITY OBSERVATION MODEL

### 2.1 Lambert Model

We first describe intensity observation model on surface of objects. We, in this paper, assume that reflectance property of the surface can be described by Lambert model. Let  $\mathbf{s}$  and  $\mathbf{n}$  denote light source direction and surface normal direction, respectively. In this case, the observed intensity  $I$  can be represented as follows:

$$I = \max(E\rho\mathbf{n}^T\mathbf{s}, 0) \quad (1)$$

where  $E$  is power of the light source and  $\rho$  is albedo of the surface. When there is no shadow on the surface, the Eq.(1) can be rewritten as follows:

$$I = E\rho\mathbf{n}^T\mathbf{s}. \quad (2)$$

The equation indicates that the normal direction  $\mathbf{n}$  can be linearly estimated from a set of intensity and a set

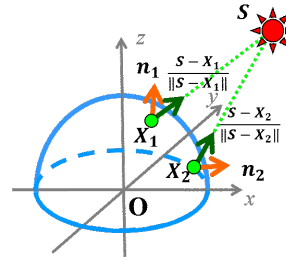


Figure 2: Relationship among a light source position  $\mathbf{S}$ , 3D point  $\mathbf{X}$  on an object surface and surface normal  $\mathbf{n}$ .

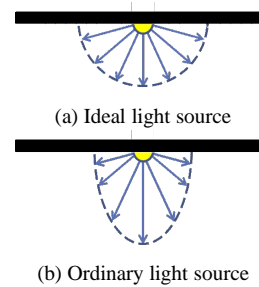


Figure 3: Light source characteristics: a light source (a) emit light rays to all direction constantly. Power of light rays from a light source (b) changes by directions of light rays.

of  $\mathbf{s}$ . This is traditional surface normal estimation by a photometric stereo method(Woodham, 1980).

### 2.2 Under Close Light Source

We next consider the case when a light source is close to the object surface. In this case, light source direction  $\mathbf{s}$  is different from each other on the surface point  $\mathbf{X}$  as shown in Fig.2. In addition, we need to consider light source characteristics since power of light ray from the light source changes by direction in ordinary case as shown in Fig.3. Especially, we use a video display device as a light source, and then, we need to consider this characteristics carefully. Therefore, intensity observation model cannot be simply described like Eq.(2). In this paper, we define the intensity model as follows:

$$\begin{aligned} I_c &= \mathcal{E} \left( \frac{\mathbf{S} - \mathbf{X}}{\|\mathbf{S} - \mathbf{X}\|} \right) \rho \frac{1}{\|\mathbf{S} - \mathbf{X}\|^2} \frac{\mathbf{n}^T(\mathbf{S} - \mathbf{X})}{\|\mathbf{S} - \mathbf{X}\|} \\ &= \mathcal{E}^{\mathbf{d}} \rho \frac{\mathbf{n}^T(\mathbf{S} - \mathbf{X})}{\|\mathbf{S} - \mathbf{X}\|^3} \end{aligned} \quad (3)$$

where  $\mathbf{S}$  is a position of the light source and  $\mathbf{X}$  is a 3D point on the surface. A function  $\mathcal{E}$  represents characteristics of light. Output of this function is changed by light ray direction  $\mathbf{d} = (\mathbf{S} - \mathbf{X})/\|\mathbf{S} - \mathbf{X}\|$ . To simplify description, the function  $\mathcal{E}((\mathbf{S} - \mathbf{X})/\|\mathbf{S} - \mathbf{X}\|)$  is written by  $\mathcal{E}^{\mathbf{d}}$ .

In this equation, a denominator of first component, i.e.  $\|\mathbf{S} - \mathbf{X}\|^2$ , indicates attenuation of the light by distance. Although the attenuation can be ignored in Eq.(2) because distance from a light source is sufficiently far, we need to consider the effect of attenuation in our model. In addition, light source characteristic  $\mathcal{E}^d$  should be considered by the same reason. Considering of these components, this intensity model become non-linear, and then, non-linear optimization must be used to estimate surface normal and object shape from a set of intensities.

### 3 LINEAR SURFACE ESTIMATION USING INTENSITY DIFFERENTIALS

#### 3.1 Intensity Differential based on Observation

In order to deal with close lighting images more easily, we focus on not only direct observed intensity by Eq.(3), but also differentials of the observed intensities.

One of the main factor of non-linearity in Eq.(3) is normalization of lighting direction  $(\mathbf{S} - \mathbf{X})$  by  $\|\mathbf{S} - \mathbf{X}\|$ . In order to avoid this explicit normalization, intensity approximation(Fujita et al., 2009) model is proposed. Although this model achieves simplifying of the equations, accuracy of the method is not high because of the approximation. In this paper, we do not use any approximation for describing the intensities. For this objective, we focus on differentials of intensities with respect to light source positions. By using the differentials, we can simplify description of intensity without any approximation.

Before explanation of our proposed model, we briefly mention measurement of intensity differentials in our system. Let  $I(\mathbf{S}_1)$  and  $I(\mathbf{S}_1 + \Delta\mathbf{S})$  denote intensities taken under a light source arranged at  $\mathbf{S}_1$  and  $\mathbf{S}_1 + \Delta\mathbf{x}(= [\Delta x, 0, 0]^T)$ . Differentials of the intensity can be described by difference of them, and then, approximated differential  $I_x(\mathbf{S})$  can be computed as follows:

$$I_x(\mathbf{S}) \sim \frac{I(\mathbf{S} + \Delta\mathbf{x}) - I(\mathbf{S})}{\Delta x} \quad (4)$$

As same as this manner,  $I_y(\mathbf{S})$  can be computed as follows:

$$I_y(\mathbf{S}) \sim \frac{I(\mathbf{S} + \Delta\mathbf{y}) - I(\mathbf{S})}{\Delta y} \quad (5)$$

In fact, these equation indicates that we need to obtain more number of images for estimating differentials. However, it is not serious problem in our system. In

our system, a video display device is used as a set of light sources, and then, the light source can be moved flexibly and quickly. Therefore, we can measure differentials of intensity quickly.

Note that we cannot measure differential of intensity wrt  $s_z$  in our system since a light sources can be moved only on the display plane.

#### 3.2 Linear Representation of Intensity and Differentials

Let us consider differentials of intensities with respect to light source positions theoretically. We first consider the case when light ray characteristics are constant, that is,  $\mathcal{E}(\mathbf{d}) = E$ . Under this assumption, Eq.(3) can be simply rewritten as follows:

$$I = E\rho \frac{\mathbf{n}^\top (\mathbf{S} - \mathbf{X})}{\|\mathbf{S} - \mathbf{X}\|^3} \quad (6)$$

Differentiating of Eq.(6), differentials  $I_x$  and  $I_y$  respect to  $s_x$  and  $s_y$  can be described as follows:

$$I_x = E\rho \frac{n_x \|\mathbf{S} - \mathbf{X}\|^2 - 3\mathbf{n}^\top (\mathbf{S} - \mathbf{X})(s_x - x)}{\|\mathbf{S} - \mathbf{X}\|^5} \quad (7)$$

$$I_y = E\rho \frac{n_y \|\mathbf{S} - \mathbf{X}\|^2 - 3\mathbf{n}^\top (\mathbf{S} - \mathbf{X})(s_y - y)}{\|\mathbf{S} - \mathbf{X}\|^5} \quad (8)$$

In addition, we rewritten Eq.(6) as follows:

$$I = E\rho \frac{\mathbf{n}^\top (\mathbf{S} - \mathbf{X}) \|\mathbf{S} - \mathbf{X}\|^2}{\|\mathbf{S} - \mathbf{X}\|^5} \quad (9)$$

In these equations, denominators of all equation are the same. Therefore, these equation can be rewritten by using homogeneous representation as follows:

$$\lambda \begin{bmatrix} I_x \\ I_y \\ I \end{bmatrix} = \begin{bmatrix} n_x \|\mathbf{S} - \mathbf{X}\|^2 - 3\mathbf{n}^\top (\mathbf{S} - \mathbf{X})(s_x - x) \\ n_y \|\mathbf{S} - \mathbf{X}\|^2 - 3\mathbf{n}^\top (\mathbf{S} - \mathbf{X})(s_y - y) \\ \mathbf{n}^\top (\mathbf{S} - \mathbf{X}) \|\mathbf{S} - \mathbf{X}\|^2 \end{bmatrix} \quad (10)$$

In this equation, denominators  $\|\mathbf{S} - \mathbf{X}\|^5$ , light source energy  $E$  and reflectance  $\rho$  are eliminated since homogeneous representation allows scale ambiguity. These components are included in all equations, and then, they are written by just  $\lambda$ . By this simplification, complicated component  $\|\mathbf{S} - \mathbf{X}\|^5$  can be ignored in this model.

#### 3.3 Linear Intensity Representation by Light Projection Matrix

We next expand these equations for linear intensity representation. In this expansion, we use constraint with  $s_z$  for simplifying the equations. In the previous section, we mentioned that a set of light sources are

on a display plane. The fact indicates that  $s_z$  can be constant in the intensity representation. In this paper, we define that  $s_z = 0$  and we expand intensity representation by using this definition.

We expand Eq.(10) and separate it into two matrices. A first matrix is a  $3 \times 8$  matrix  $\mathbf{P}$  based on object shape  $\mathbf{X}$  and surface normal  $\mathbf{n}$ . This matrix  $\mathbf{P}$  is described as follows:

$$\mathbf{P} = \begin{bmatrix} 0 & 0 & -2n_x & n_x & & & & \\ 0 & 0 & n_y & -2n_y & & & & \\ n_x & n_y & -(\mathbf{n}^\top \mathbf{X} + 2n_y y) & -(\mathbf{n}^\top \mathbf{X} + 2n_x x) & & & & \\ & -3n_y & 3\mathbf{n}^\top \mathbf{X} - n_x x & & & & & \\ & -3n_x & -2n_y x + 3n_x y & & & & & \\ -2(n_y x + n_x y) & n_x \mathbf{X}^\top \mathbf{X} + 2x \mathbf{n}^\top \mathbf{X} & & & & & & \\ & 3n_y x - 3n_x y & n_x \mathbf{X}^\top \mathbf{X} - 3x \mathbf{n}^\top \mathbf{X} & & & & & \\ & 3\mathbf{n}^\top \mathbf{X} + n_y y & n_y \mathbf{X}^\top \mathbf{X} - 3y \mathbf{n}^\top \mathbf{X} & & & & & \\ n_y \mathbf{X}^\top \mathbf{X} + 2y \mathbf{n}^\top \mathbf{X} & & \mathbf{n}^\top \mathbf{X} \mathbf{X}^\top \mathbf{X} & & & & & \end{bmatrix} \quad (11)$$

The next component is an 8-dimensional vector  $\mathbf{L}$  based on light source position  $\mathbf{S}$  and it is described as follows:

$$\mathbf{L} = [ s_x^5 + s_x s_y^2 \quad s_y^3 + s_x^2 s_y \quad s_x^2 \quad s_y^2 \quad s_x s_y \quad s_x \quad s_y \quad 1 ]^\top \quad (12)$$

By using  $\mathbf{P}$  and  $\mathbf{L}$ , set of intensity  $[I, I_x, I_y]^\top$  can be represented linearly as follows:

$$\lambda \begin{bmatrix} I \\ I_x \\ I_y \end{bmatrix} \mathbf{I} = \mathbf{P} \mathbf{L} \quad (13)$$

By using this representation, we can describe changes of intensity depends on position of a light source linearly. In this paper,  $\mathbf{P}$  and  $\mathbf{L}$  are called light projection matrix and light information vector respectively.

### 3.4 Linear Shape Estimation

We next consider linear estimation of object shape. In fact, light projection matrices include object shape  $\mathbf{X}$  and surface normal  $\mathbf{n}$  directly, and then, the components can be computed easily when the light projection matrix can be estimated. Therefore, we explain estimation method of the matrix  $\mathbf{P}$ .

Let  $\mathbf{L}_i$  and  $\mathbf{I}_i$  denote a light information vector and observed intensities under  $i$ -th ( $i = 1, \dots, N$ ) light source position. In this case, Eq. (13) can be rewritten as follows:

$$\lambda_i \mathbf{I}_i = \mathbf{P} \mathbf{L}_i \quad (14)$$

where  $\lambda_i$  is a scale ambiguity. For eliminating this ambiguity, we transform the equation by using skew symmetric matrix  $[\mathbf{I}]_\times$  as follows:

$$[\mathbf{I}]_\times \mathbf{I}_i = \lambda_i [\mathbf{I}]_\times \mathbf{P} \mathbf{L}_i = \mathbf{0} \quad (15)$$

When  $\lambda_i$  is not 0, the  $\lambda_i$  can be eliminated by dividing by itself. Therefore, we can obtain linear constraint from  $N$  images as follows:

$$\begin{bmatrix} \mathbf{L}_1^\top [\mathbf{I}_1]_\times \\ \vdots \\ \mathbf{L}_N^\top [\mathbf{I}_N]_\times \end{bmatrix} \mathbf{P}^\top = \mathbf{0} \quad (16)$$

By solving this equations, the light projection matrix  $\mathbf{P}$  can be estimated. This solution can be provided by ordinary least means square method since they are just linear equations. That is, linear estimation of object shape is achieved without any approximation.

## 4 INTENSITY REPRESENTATION WITH LIGHT SOURCE CHARACTERISTICS

### 4.1 Intensity Differential with Characteristic

In this section, we consider linear intensity representation with light source characteristics. In this case, light source energy  $E$  in all equations are replaced to light source characteristics  $\mathcal{E}^d$ . The characteristic function  $\mathcal{E}^d$  depends on  $\mathbf{S}$ , and then,  $\mathcal{E}^d$  changes by changing of  $\mathbf{S}$ . Therefore, we need to reflect this effect to differentials of intensities.

In fact, this reflection is not so difficult since  $\mathcal{E}^d$  is just multiplier. By using observed intensity  $I$  and power of light  $E$  in Eq.(6), observed intensity  $I'$  which includes characteristics  $\mathcal{E}^d$  can be described as follows:

$$I' = \mathcal{E}^d \rho \frac{\mathbf{n}^\top (\mathbf{S} - \mathbf{X}) \|\mathbf{S} - \mathbf{X}\|^2}{\|\mathbf{S} - \mathbf{X}\|^5} = \mathcal{E}^d \frac{I}{E} \quad (17)$$

As same as this manner, differentials  $I'_x$  and  $I'_y$  can be described by  $I_x$  and  $I_y$  as follows:

$$I'_x = \mathcal{E}^d \frac{I_x}{E} + \mathcal{E}_x^d \frac{I}{E} \quad (18)$$

$$I'_y = \mathcal{E}^d \frac{I_y}{E} + \mathcal{E}_y^d \frac{I}{E} \quad (19)$$

where  $\mathcal{E}_x^d$  and  $\mathcal{E}_y^d$  are differentials of light source characteristic with respect to  $s_x$  and  $s_y$  respectively. Therefore, observed set of intensities  $\mathbf{I}'$  including  $\mathcal{E}^d$  can be described as follows:

$$\mathbf{I}' = \frac{1}{E} \begin{bmatrix} \mathcal{E}^d & 0 & \mathcal{E}_x^d \\ 0 & \mathcal{E}^d & \mathcal{E}_y^d \\ 0 & 0 & \mathcal{E}^d \end{bmatrix} \begin{bmatrix} I_x \\ I_y \\ I \end{bmatrix} = \mathbf{E}^d \mathbf{P} \mathbf{L} \quad (20)$$

where  $\mathbf{E}$  includes light source characteristics and its differentials. By using these equations, images taken under close light source can be described linearly even if light source characteristic is not constant.

## 4.2 Shape Estimation with Characteristic

We next consider shape reconstruction by Eq.(20). At glance, light projection matrix  $\mathbf{P}$  can be estimated by the same way to Eq.(16) which does not include  $\mathbf{E}$ . However, we cannot utilize this method because  $\mathcal{E}$  depends on not only light source position  $\mathbf{S}$ , but also reconstructed shape  $\mathbf{X}$ . Therefore, we use iterative estimation method for estimating a projection matrix  $\mathbf{P}$ .

In this iterative method, we first provide initial light source direction  $\mathbf{d} = [0, 0, 1]^\top$  for each point. From the initial direction,  $\mathbf{E}_0$  can be computed directly. When  $\mathbf{E}_0$  is obtained from it, we can estimate  $\mathbf{P}$  linearly under the characteristics as follows:

$$\begin{bmatrix} \mathbf{L}_1^\top [\mathbf{E}_0^{-1} \mathbf{I}_1]_\times \\ \vdots \\ \mathbf{L}_N^\top [\mathbf{E}_0^{-1} \mathbf{I}_N]_\times \end{bmatrix} \mathbf{P}_0^\top = \mathbf{0} \quad (21)$$

From this equation, object shape  $\mathbf{X}_0$  based on  $\mathbf{P}_0$  can be estimated, and then, a direction  $\mathbf{d}_0$  can be updated to  $\mathbf{d}_1$  as follows:

$$\mathbf{d}_1 = \frac{\mathbf{S} - \mathbf{X}_0}{\|\mathbf{S} - \mathbf{X}_0\|} \quad (22)$$

From this updated direction,  $\mathbf{E}_0$  can be also updated to  $\mathbf{E}_1$ . Therefore, a projection matrix  $\mathbf{P}_i$  for  $i$ -th iteration can be estimated as follows:

$$\begin{bmatrix} \mathbf{L}_1^\top [\mathbf{E}_i^{-1} \mathbf{I}_1]_\times \\ \vdots \\ \mathbf{L}_N^\top [\mathbf{E}_i^{-1} \mathbf{I}_N]_\times \end{bmatrix} \mathbf{P}_i^\top = \mathbf{0}$$

We finally obtain appropriate shape  $\mathbf{X}$  and surface normal  $\mathbf{n}$  based on matrix  $\mathbf{P}$ .

Note that, we can obtain not only surface normal  $\mathbf{n}$ , but also object shape  $\mathbf{X}$  from the estimated projection matrix  $\mathbf{P}$ . However, accuracy of estimated  $\mathbf{X}$  is not better since effect of surface normal  $\mathbf{n}$  is stronger than effect of  $\mathbf{X}$  in observed intensities. Therefore, we have to combine these two estimated result for more accurate estimation. In this combining, surface normal  $\mathbf{n}$  is integrated to object shape around estimated shape  $\mathbf{X}$ . By using direct shape estimation result  $\mathbf{X}$  in this integration, we can reconstruct object shape even if the object includes discontinuous surface. By using both two components, our method can reconstruct object shape accurately and stably.



Figure 4: Display characteristics measurement: light source on the display moved, and changes of intensities on the cube were measured.

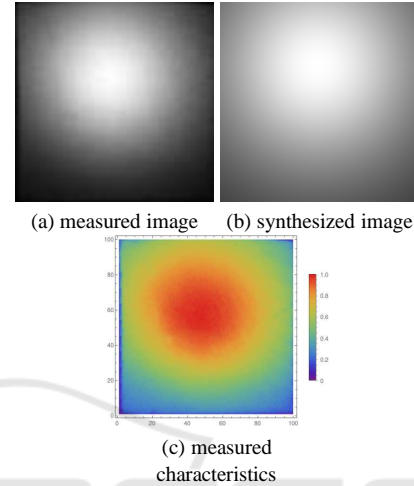


Figure 5: Three images for measuring light source characteristic: (a) is measured image, (b) is synthesized image taken under ideal light source and (c) is estimated  $\mathcal{E}$  from (a) and (b).

## 5 EXPERIMENTAL RESULTS

### 5.1 Measurement of Light Source Characteristics

Let us show some experimental result by our proposed method. We first show measurement result of display (light source) characteristics for validating our proposed intensity model by Eq.(3). In this measurement, we set up a display device and a plaster cube which had Lambert surface as shown in Fig.4. A light source on the display was moved and images were taken under each light source position. An example of taken image is shown in Fig.5(a). For estimating  $\mathcal{E}^{\mathbf{d}}$ , distance between the display and the light source was measured directly, and an image taken under ideal (constant) light source characteristics was synthesized as shown in Fig.5(b) by Eq.(6). From these images, light source characteristics  $\mathcal{E}^{\mathbf{d}}$  of each pixel was estimated as shown in Fig.5(c). By integration of estimated  $\mathcal{E}^{\mathbf{d}}$  taken under different light source position, the whole characteristic  $\mathcal{E}^{\mathbf{d}}$  is estimated. The esti-

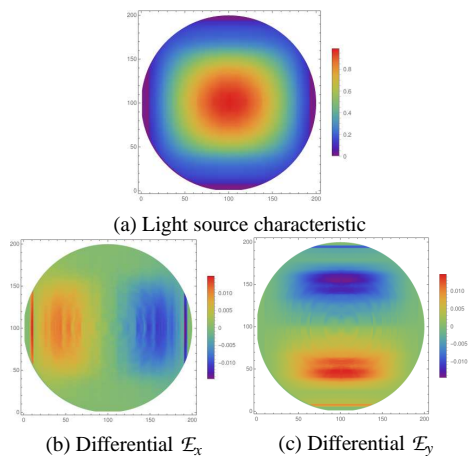


Figure 6: Measured light source characteristics:(a) shows direct characteristic  $\mathcal{E}$  and (b),(c) show differentials  $\mathcal{E}_x$  and  $\mathcal{E}_y$  respectively.

imated result is shown in Fig.6(a) and differentials  $\mathcal{E}_x$  and  $\mathcal{E}_y$  is also shown in Fig6(b) and (c). In these figures, a direction vector  $\mathbf{d}$  is parallel projected onto  $xy$ -plane, i.e.  $\mathcal{E}([d_x, d_y, d_z]^T)$  is represented at a point  $(d_x, d_y)$ . These results indicate that characteristics of the provided display is not constant obviously. That fact indicates Eq.(9) is not sufficient to represent observed intensities taken under the display. Therefore, we need to utilize Eq.(3) to represent intensities and estimate object shape accurately.

## 5.2 Environment

We next show shape reconstruction result by using our proposed method. We describe experimental environment at first. In this experiment, we constructed experimental environment in computers and synthesized images in this simulation environment. Figure7 shows target objects for shape reconstruction. The target (b) includes discontinuous surface which cannot be differentiated. These objects are illuminated by a display in the scene. Light source characteristics measured in 5.1 was utilized for characteristics of this display. By using the display illumination, input images were synthesized under 100 different light source positions. Several examples of the images are shown in Fig.8. From these images, differentials of intensity were computed and object shape was reconstructed by our proposed method. For comparison, object shape was also reconstructed by an traditional photometric stereo method. In this method, surface normal were reconstructed under infinite light source assumption and shape was estimated by integration of the surface normal.

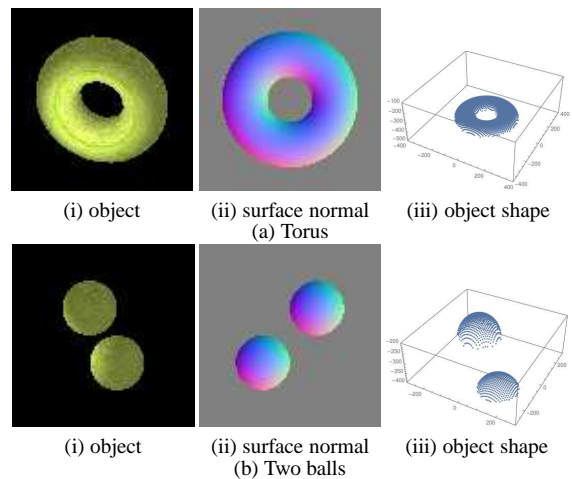


Figure 7: Target objects: (a) Torus and (b) two balls.

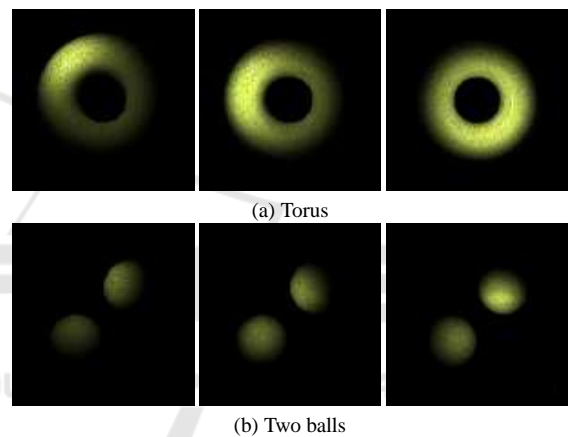


Figure 8: Examples of synthesized images.

## 5.3 Results

Reconstructed results of a torus are shown in Fig.9. In this figure, reconstructed surface normal and reconstructed shape are compared to a result by an traditional photometric stereo method. These figure indicates that although surface normal can be estimated by our proposed method, it cannot be reconstructed by the traditional method because the method cannot represent changes of light source direction, light source characteristics, and intensity attenuation by distance accurately. In shape reconstruction result, although direct estimation result shown in Fig.9(v) is not so accurate, the accuracy can be improved drastically by combining surface normal estimation result and object shape reconstruction result as shown in Fig.9(vi). This is because the accuracy of surface normal estimation is higher than object shape estimation. On the other hand, reconstructed shape by the traditional method is not accurate since surface normal cannot be

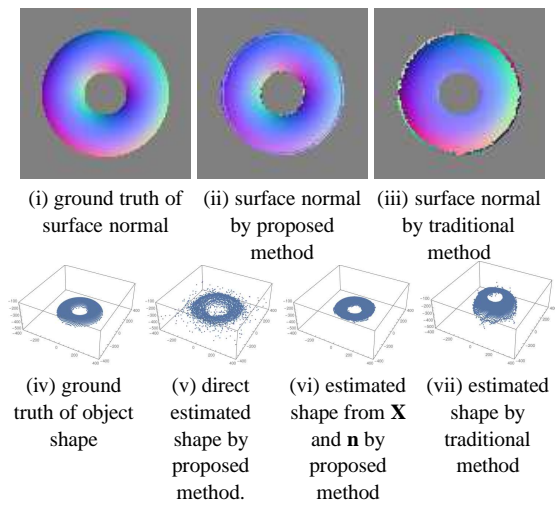


Figure 9: Reconstructed result of torus: (i), (ii) and (iii) show (i) ground truth of surface normal, (ii) estimated result by our proposed method and (iii) estimated result by traditional method. (iv)~(vii) show (iv) ground truth of object shape, (v) direct estimated shape from  $\mathbf{P}$  by our method, (vi) final reconstructed shape using  $\mathbf{n}$  and  $\mathbf{X}$  and (vii) reconstructed shape by traditional method.

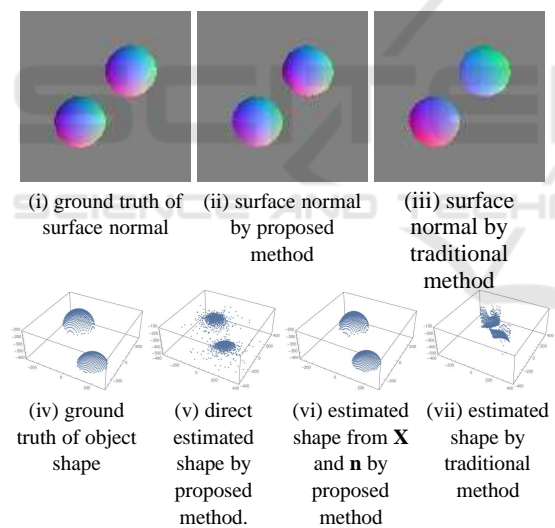


Figure 10: Reconstructed result of two balls.

estimated accurately with their assumptions.

Figure 10 shows estimated results of two balls. In this result, although our method can reconstruct surface normal and object shape accurately, the traditional method cannot reconstruct them. Especially, as shown in Fig.10(vi), shape of the two balls can be estimated validly by our method even if two balls have different depth from each other. In our method, direct shape estimation results and integrated surface normal are combined for estimating object shape, and then, discontinuous surface can be reconstructed correctly.

These results indicate that our method can reconstruct object shape and surface normal accurately. That is, our linear intensity representation based on intensity differentials is effective for shape estimation from images taken under close light sources.

## 6 CONCLUSIONS

In this paper, we propose a new linear photometric stereo method based on differentials of image intensities. In this method, not only direct observed intensity, but also differentials of intensities are used for linear representation of the intensities. By using the linear intensity representation, object shape can be also linearly estimated. In addition, not only surface normal of the object, but also object shape can be estimated directly. Furthermore, accurate object shape can be reconstructed by combining estimated shape and surface normal even if the target shape includes discontinuous surface. As a result, we achieve quick and compact 3D measurement system by using a video display as a set of light sources. In our proposed 3D measurement system, special devices for 3D measurement are not required and we need to prepare only an ordinary display and a camera.

## REFERENCES

Brostow, G., Hernandez, C., Vogiatzis, G., Stenger, B., and Cipolla, R. (2011). Video normals from colored lights. *Trans. PAMI*, 33(10):2104–2114.

Chen, C., Vauero, D., and Turk, M. (2011). Illumination demultiplexing from a single image. In *Proc. ICCV2011*, pages 17–24.

Fujita, Y., Sakau, F., and Sato, J. (2009). Linear image representation under close lighting for shape reconstruction. In *Proc. International Conference on Computer Vision Theory and Applications*, volume 2, pages 67–72.

Hayakawa, H. (1994). Photometric stereo under a light source with arbitrary motion. *Journal of the Optical Society of America A*, 11(11):3079–3089.

Iwahori, Y. (1990). Reconstructing shape from shading images under point light source illumination. In *Proc. of International Conference on Pattern Recognition (ICPR'90)*, pages 83–87.

Kato, K., Sakau, F., and Sato, J. (2010). Extended multiple view geometry for lights and cameras from photometric and geometric constraints. In *Proc. 12th International Conference on Pattern Recognition (ICPR2010)*, pages 2110–2113.

Kim, B. and Burger, P. (1991). Depth and shape from shading using the photometric stereo method. *CVGIP: Image Understanding*, 54(3):416–427.

- Okabe, T. and Sato, Y. (2006). Effects of image segmentation for approximating object appearance under near lighting. *Proc. of Asian Conference on Computer Vision (ACCV2006)*, I:764–775.
- Woodham, R. (1980). Photometric method for determining surface orientation from multiple images. *Optical Engineerings*, 19(1):139–144.

